Method

A network-based analysis of colon cancer splicing changes reveals a tumorigenesis-favoring regulatory pathway emanating from ELK1

Dror Hollander,[1] Maya Donyo,[1,7] Nir Atias,[2,7] Keren Mekahel,[1] Zeev Melamed,[1,8] Sivan Yannai,[1] Galit Lev-Maor,[1] Asaf Shilo,[3] Schraga Schwartz,[4] Iris Barshack,[5,6] Roded Sharan,[2] and Gil Ast[1]

[1]Department of Human Molecular Genetics and Biochemistry, Sackler Faculty of Medicine, Tel Aviv University, Ramat Aviv 69978, Israel; [2]Blavatnik School of Computer Science, Tel Aviv University, Ramat Aviv 69978, Israel; [3]Department of Biochemistry and Molecular Biology, Institute for Medical Research Israel-Canada, The Hebrew University-Hadassah Medical School, Jerusalem 91120, Israel; [4]Department of Molecular Genetics, Weizmann Institute, Rehovot 76100, Israel; [5]Department of Pathology, Sheba Medical Center, Ramat Gan 52621, Israel; [6]Sackler Faculty of Medicine, Tel Aviv University, Ramat Aviv 69978, Israel

Splicing aberrations are prominent drivers of cancer, yet the regulatory pathways controlling them are mostly unknown. Here we develop a method that integrates physical interaction, gene expression, and alternative splicing data to construct the largest map of transcriptomic and proteomic interactions leading to cancerous splicing aberrations defined to date, and identify driver pathways therein. We apply our method to colon adenocarcinoma and non-small-cell lung carcinoma. By focusing on colon cancer, we reveal a novel tumor-favoring regulatory pathway involving the induction of the transcription factor MYC by the transcription factor ELK1, as well as the subsequent induction of the alternative splicing factor PTBP1 by both. We show that PTBP1 promotes specific RAC1, NUMB, and PKM splicing isoforms that are major triggers of colon tumorigenesis. By testing the pathway's activity in patient tumor samples, we find ELK1, MYC, and PTBP1 to be overexpressed in conjunction with oncogenic KRAS mutations, and show that these mutations increase ELK1 levels via the RAS-MAPK pathway. We thus illuminate, for the first time, a full regulatory pathway connecting prevalent cancerous mutations to functional tumor-inducing splicing aberrations. Our results demonstrate our method is applicable to different cancers to reveal regulatory pathways promoting splicing aberrations.

[Supplemental material is available for this article.]

Alternative splicing is an evolutionarily conserved mechanism that increases transcriptomic and proteomic diversity by allowing the generation of multiple mRNA products from a single gene. It is highly prevalent as >95% of human multiexonic genes undergo alternative splicing (Pan et al. 2008; Wang et al. 2008b). Numerous exonic and intronic cis-acting sequences can either enhance or repress splicing unit recognition pending on binding of trans-acting alternative splicing factors (Guigo and Valcarcel 2006). One of these factors is the polypyrimidine tract-binding protein PTBP1 (previously known as PTB). PTBP1 is a heterogeneous nuclear ribonucleoprotein that binds RNA via four domains of varying functionality (Mickleburgh et al. 2014) and can act as a repressive or as an enhancing alternative splicing regulator (Xue et al. 2009; Keppetipola et al. 2012).

Three main types of evidence have established a strong connection between alternative splicing and cancer development. First, several alternative splicing factors, such as SRSF1, RBFOX2, PTBP1, HNRNPA1, HNRNPA2B1, and SRSF6, are overexpressed in different cancer tissues and display oncogenic properties (Karni et al. 2007; Cooper et al. 2009; Venables et al. 2009; David

and Manley 2010; Golan-Gerstl et al. 2011; Cohen-Eliav et al. 2013). Second, changes in the splicing patterns of various alternative splicing events were identified in tumors in comparison with their corresponding normal tissues (Kim et al. 2008; Liu et al. 2012; Pesson et al. 2014), and some were demonstrated to play prominent roles in carcinogenesis (Srebrow and Kornblihtt 2006; Wang and Cooper 2007; Papasaikas et al. 2015). Third, splicing factors, such as SF3B1 and U2AF1, are highly mutated in several malignancies (Graubert et al. 2011; Quesada et al. 2012). However, the underlying causes of the cancerous up-regulation of alternative splicing factors as well as the specific inducers of splicing aberrations in tumors are still largely unknown.

Colon and rectal tumors constitute a major cause of cancer mortality, as an estimated 1 million individuals worldwide develop them yearly with a disease mortality rate of ~33% in the developed world (Cunningham et al. 2010). The molecular mechanism in colon tumorigenesis is largely nonhereditary and is mainly triggered by a series of oncogene-activating mutations and tumor suppressor gene–deactivating mutations in a relatively small set of genes (Fearon 2011). The most prevalent are those

found in *APC*, *KRAS*, and *TP53* (Wood et al. 2007; Fearon 2011). Mutations in these genes lead to up-regulation of the Wnt and RAS-MAPK signaling pathways and to down-regulation of the TP53 pathway, resulting in the overexpression of the oncogenic transcription factor MYC, increased cell proliferation, and, eventually, colon carcinogenesis (Fearon 2011; The Cancer Genome Research Atlas Network 2012b).

Several alternative splicing events have been reported to display different splicing patterns in colon tumors compared with the normal tissue. Three noteworthy splicing pattern differences are the inclusion of *RAC1* exon 3b, the increased inclusion of *NUMB* exon 9, and the inclusion of *PKM* exon 10 in conjunction with exon 9 exclusion (Jordan et al. 1999; Hardt et al. 2003; Misquitta-Ali et al. 2010). These specifically contribute to colon tumorigenesis through proteomic changes that cause Notch pathway activation and promotion of aerobic glycolysis, genomic instability, and epithelial–mesenchymal transition (Radisky et al. 2005; Christofk et al. 2008; Misquitta-Ali et al. 2010; Bechara et al. 2013; Myant et al. 2013). In addition, PRPF6, a member of the tri-snRNP (small ribonucleoprotein) spliceosome complex, was shown to positively affect colon cancer proliferation (Adler et al. 2014).

Several pathways involving transcription factor activity affecting alternative splicing factors have been shown to undergo overactivation or disruption in different cancer types, thus contributing to carcinogenesis (David and Manley 2010; Das et al. 2012). Nevertheless, current knowledge concerning alternative splicing regulation in cancer leaves much to be desired, calling for a systematic examination of the pathways leading to cancerous splicing aberrations.

Results

Constructing a physical interaction network underlying cancerous splicing aberrations

Deciphering the regulation of alternative splicing in cancer is fundamental to our understanding of the disease processes and ways to combat them. To study the pathways that govern alternative splicing factor activity and, subsequently, splicing changes in cancer, we integrated large-scale protein–DNA, protein–RNA, and protein–protein physical interaction data together with gene expression and alternative splicing data into a single network (Methods). Briefly, we analyzed high-throughput cross-linking and immunoprecipitation (CLIP) data of human alternative splicing factors (Sanford et al. 2009; Xiao et al. 2009; Xue et al. 2009; Yeo et al. 2009; Hafner et al. 2010; Konig et al. 2010; Wang et al. 2010; Kishore et al. 2011; Lebedeva et al. 2011; Mukherjee et al. 2011; Tollervey et al. 2011; Huelga et al. 2012) to determine their protein–pre-mRNA interactions in regions encompassing all internal exons in multiexonic genes and 300-bp-long flanking intronic regions (15,501 interactions in total). In addition, 16,320 human protein–DNA interactions between transcription factors and the genes they bind, as well as 45,055 protein–protein interactions, were derived from chromatin immunoprecipitation (ChIP), yeast two-hybrid, and coimmunoprecipitation screens, as well as from publicly available databases (Yosef et al. 2011; Hegele et al. 2012). All interactions were assigned confidence scores as previously described (Yosef et al. 2011). This combined network is a powerful resource linking three regulatory layers, which are likely to work in coordination in the context of a biological process of interest. It is available through ANAT (Yosef et al. 2011), a free

Cytoscape (Saito et al. 2012) plug-in for network analysis (http://www.cs.tau.ac.il/~bnet/ANAT). An initial examination of alternative splicing factor protein–protein interaction data in our network revealed a distinct module of interacting factors that includes several cancer-associated proteins (Supplemental Fig. S1; Supplemental Results).

To focus on splicing aberrations in cancer, we analyzed transcriptome-wide data of cancerous and normal tissues spanning 24,426 alternative splicing events and 18,093 genes (Castle et al. 2008), identifying alternative splicing events that exhibit significant splicing differences in tumors compared with corresponding normal tissues (Methods). We then searched the combined network for high-confidence subnetworks connecting transcription factors with the determined differentially spliced events in tumors (schematically depicted in Fig. 1A). The search algorithm builds upon a previously described method by Yosef et al. (2009) and additionally assigns significance values to each inferred subnetwork that reflect the gene expression changes of its members in cancer. Briefly, the algorithm jointly optimizes the size of the inferred subnetwork, the confidence of its member interactions, and the confidence of each of the paths connecting a transcription factor to a differentially spliced event. Significance levels are calculated according to the cancerous gene expression changes in the inferred subnetwork in comparison with the normal tissue gene expression (Methods). The resulting subnetworks coherently describe significant regulatory pathways that emanate from a transcription factor and are likely to induce splicing aberrations.

Network leading to colon cancer splicing changes emanates from ELKI

We applied our method to construct the splicing interactomes of colon adenocarcinoma and lung squamous cell carcinoma NOS (Fig. 1B; Supplemental Fig. S2, respectively) using transcriptomic data of tumors and normal tissues (Castle et al. 2008). Interestingly, the constructed subnetworks were significantly enriched for cancer-associated Kyoto Encyclopedia of Genes and Genomes (KEGG) pathways (Kanehisa et al. 2012) and genes included in the Catalogue of Somatic Mutations in Cancer (COSMIC; Forbes et al. 2011), two gold standard references for the evaluation of cancerous gene and protein annotations (Supplemental Table S1). Focusing on colon cancer, the only significant subnetwork was that originating in ELK1 (Methods), a member of the oncogenic ETS family of transcription factors. The network reveals a pathway involving ELK1, MYC, and PTBP1, accounting for the majority of alternatively spliced events. Intriguingly, PTBP1 is an alternative splicing factor previously shown to be overexpressed in brain tumors and implicated in their formation (David et al. 2010). It has also been suggested to be involved in breast cancer epithelial–mesenchymal transition (Shapiro et al. 2011; He et al. 2014). In the pathway we identified, ELK1 directly regulates the gene expression of *PTBP1* and *MYC*, an oncogenic transcription factor that plays an important role in colon tumor development (Fearon 2011). Downstream from ELK1, MYC also directly regulates the transcriptional induction of *PTBP1* as well as that of *HNRNPF*, an alternative splicing factor shown to be overexpressed in colon cancer (Balasubramani et al. 2006). *PTBP1* up-regulation by MYC is known to promote lung tumor formation (Clower et al. 2010; David et al. 2010), but the addition of *MYC* activation by ELK1 and the MYC-independent activation of *PTBP1* by ELK1 have not been previously reported in the context of cancer formation.
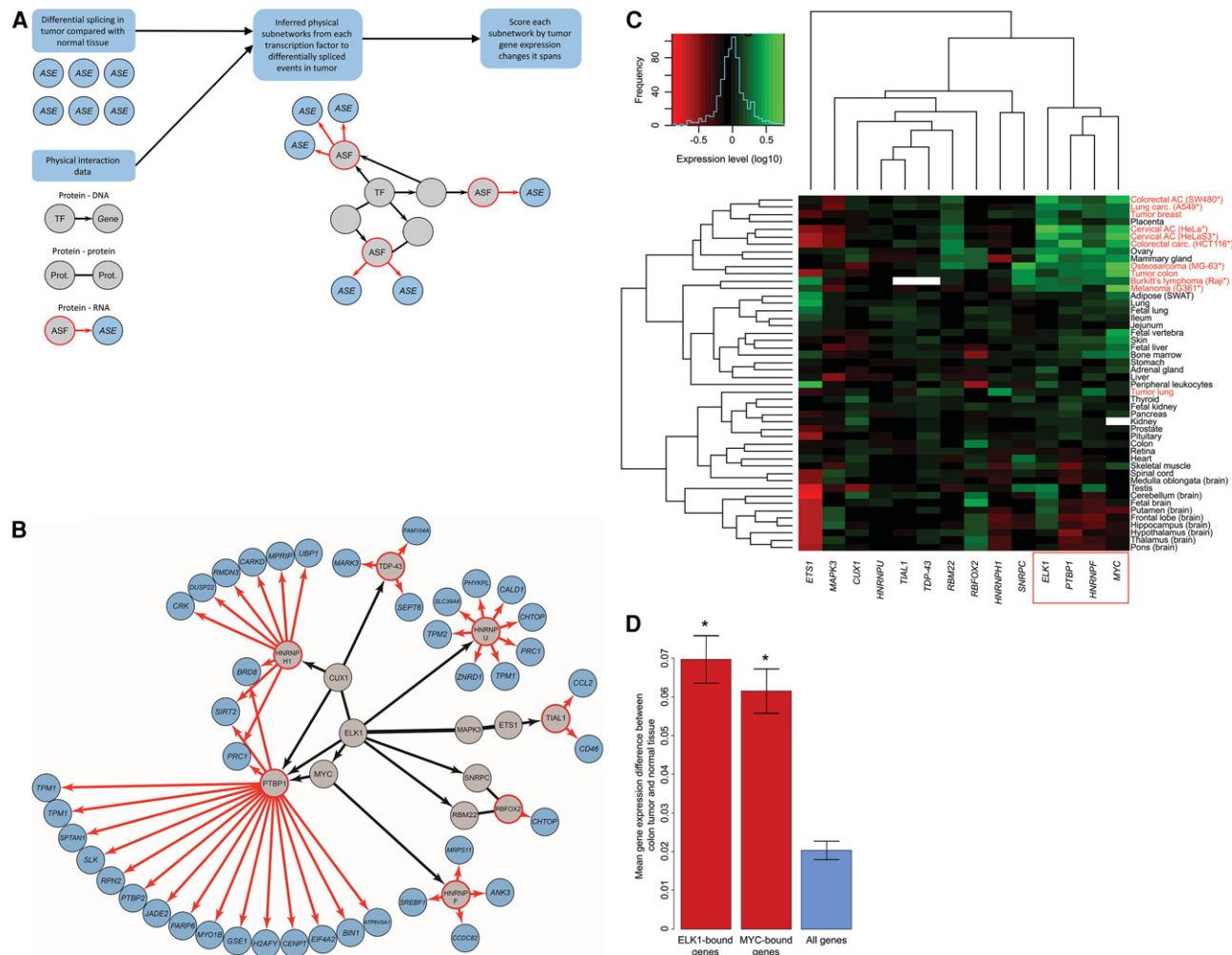
Figure 1. Physical interaction network leading to colon cancer splicing changes. (A) A diagram illustrating the construction of the cancerous splicing interactome connecting transcription factors (TFs) to alternative splicing events (ASEs) exhibiting splicing pattern differences in tumors compared with normal tissues (alternative splicing factor [ASF]). (B) ELK1 colon tumor subnetwork. Gene names of exons exhibiting significant splicing changes in the colon tumor compared with the normal tissue are colored light blue; all other genes and proteins are colored gray. Alternative splicing factors are marked by red borders. Protein–DNA and protein–pre-mRNA interactions are marked by black and red directed arrows, respectively. (C) Hierarchical clustering of ELK1 subnetwork member gene expression in 48 human tissue and cell lines. Tumor and cancer cell line names are colored red. Cell lines are marked by an asterisk. White boxes denote missing reads. The color key legend includes a histogram of the gene expression level distribution. (D) Mean gene expression level difference between colon tumor and normal tissue of genes with promoters bound by ELK1 ($n = 1937$), genes with promoters bound by MYC ($n = 3226$), and all genes ($n = 18,093$); arbitrary units. Error bars, SEM.

Colon cancer up-regulation of ELK1, MYC, and their target genes

To support the identified regulatory pathway in the ELK1 subnetwork, we analyzed the subnetwork's gene expression profile using transcriptome-wide data spanning 48 human tissues and cell lines, including the colon tumor, cell lines derived from it, and the corresponding normal colon (Fig. 1C; Castle et al. 2008). Our results demonstrate that a gene cluster including *ELK1*, *MYC*, *PTBP1*, and *HNRNPF* exhibits similar gene expression levels. This cluster substantially differs in its expression pattern from other network members and, most importantly, is up-regulated in several tumors and cancer cell lines, including the colon tumor. To test whether ELK1 and MYC are overactive in colon cancer compared with the normal colon, we examined the gene expression changes of their targets. ELK1 and MYC ChIP coupled with high-throughput sequencing (ChIP-seq) data (obtained from the ENCODE Project Consortium 2012) were analyzed to identify high-confidence

read peaks of gene promoters bound by the proteins (Methods). We then measured the mean difference in the expression level of these genes between tumor and normal colon tissues (Fig. 1D). ELK1-bound and MYC-bound genes exhibited significantly higher mean differences in expression levels compared with all genes (two-sided Student's t-test; $P = 9.67 \times 10^{-14}$ and $P = 2.35 \times 10^{-11}$, respectively), implying that ELK1 and MYC are indeed overactive in colon cancer. Overall, these results reinforce the identified regulatory pathway involving ELK1 and MYC, which could be implicated in colon cancer formation.

PTBP1, *RBFOX2*, *HNRNPH1*, and *HNRNPF* expression levels are positively correlated with cancer-associated splicing isoforms their proteins bind

In a previous work, we demonstrated a correlative relationship between the gene expression of an alternative splicing factor and the

splicing events it regulates (Llorian et al. 2010). To examine such relations in the context of the ELK1 subnetwork, we tested whether the gene expression levels of alternative splicing factors identified in the subnetwork were correlated with the splicing changes of exons their proteins bind. All high-throughput CLIP-derived peaks located in the vicinity of differentially spliced exons in the colon tumor compared with the normal colon were used in the analysis. We found that four of the seven alternative splicing factors in the ELK1 subnetwork—*PTBP1*, *RBFOX2*, *HNRNPH1*, and *HNRNPF*—exhibit strong positive correlations (Fig. 2A). Of these, *PTBP1*, the alternative splicing factor that interacts with the highest number of differentially spliced events in the subnetwork, also displays the strongest correlations with the alternative exons bound by it (mean $R = 0.51$). This indicates that PTBP1 may promote production of these cancerous splicing isoforms. The strong correlations exhibited by *RBFOX2* (mean $R = 0.5$) are in accordance with evidence suggesting that this factor drives mesenchymal tissue–specific splicing in both tumors and normal tissues (Venables et al. 2013). Furthermore, analyses of tissue-specific patterns of alternative splicing and the gene expression levels of alternative splicing factors revealed similar tissue clusters, including one consisting of several tumors and cancer cell lines (Supplemental Fig. S3; Supplemental Results), further suggesting that alternative splicing factor transcriptional changes in cancer may play a role in bringing forth cancerous alternative splicing programs.

In silico identification of colon cancer alternative splicing regulators

Based on our findings, we hypothesized that the relationship between splicing changes and alternative splicing factor gene expression could be used to identify additional factors that regulate splicing aberrations in colon cancer, for which high-throughput CLIP data are currently unavailable. Moreover, not all possible RNA targets are identified within a single high-throughput CLIP experiment as the purified RNA molecules in it only correspond to RNAs bound at the moment of cross-linking (Kloetgen et al. 2014). Our analysis could therefore determine additional regulatory targets (see Supplemental Discussion). To this end, we compiled a list of 54 experimentally validated alternative splicing events shown to undergo a splicing pattern change in colon tumor samples compared with corresponding normal tissue samples (Jordan et al. 1999; Hardt et al. 2003; Ghigna et al. 2005; Gardina et al. 2006; Klinck et al. 2008; Thorsen et al. 2008; Venables et al. 2009; Langer et al. 2010; Misquitta-Ali et al. 2010; Pio et al. 2010; Choi et al. 2011; Ishimoto et al. 2011; Liu et al. 2012; Miura et al. 2012; Seo et al. 2012). We then identified the potential regulators of these cancerous splicing changes by the number and strength of determined Pearson correlations between the splicing changes of the 54 alternative events across 48 human tissues and cell lines and the gene expression of alternative splicing factors in the same tissues (Methods). The mean coefficient values of the five highest ranking alternative factors are depicted in Figure 2B.

Here, too, *PTBP1* exhibited the strongest relations with the highest number of alternative splicing events (mean $R = 0.53$). It is predicted to induce the cancerous isoform of 13 alternative events, 10 of which lack significant CLIP-seq read peaks (Fig. 2C,D; data not shown). Reassuringly, PTBP1 has been shown to regulate four of the predicted targets in the *PKM*, *TPM1*, *ACTN1*, and *ATP2B4* genes in other tissues (Clower et al. 2010; Llorian et al. 2010; Mallinjoud et al. 2014). In accordance with Figure

2A, *HNRNPF* displayed strong correlations with colon cancer splicing patterns (mean $R = 0.44$). The *QKI* and *CELF2* alternative splicing factors exhibited the strongest negative relations with colon cancer splicing patterns (mean $R = −0.47$). Interestingly, the expression of both proteins has been reported to induce a tumor-suppressing effect (Ramalingam et al. 2012; Zong et al. 2014). Our results therefore indicate that PTBP1 could play a previously unknown role in promoting a number of colon cancer alternative splicing changes, while QKI and CELF2 may have an opposite effect.

PTBP1 promotes colon tumorigenesis-triggering splicing isoforms

To validate PTBP1's regulatory role in inducing cancerous splicing aberrations in the colon based on our analysis (Fig. 2B), RNA interference-mediated (siRNA) knockdown of *PTBP1* and of *PTBP2* (previously known as *nPTB*), its functionally redundant paralog (Spellman et al. 2007), was performed in the HCT116 colorectal carcinoma cell line. Splicing pattern changes of PTBP1's predicted targets after siRNA treatment were examined via RT-PCR. Upon treatment with the control siRNA, all examined alternative splicing events displayed the same splicing patterns as those originally identified in the tumor samples (Fig. 2C,D; Supplemental Fig. S4A, B, and data not shown; Jordan et al. 1999; Hardt et al. 2003; Gardina et al. 2006; Thorsen et al. 2008; Misquitta-Ali et al. 2010). Overall, 11 of 13 (85%) predicted PTBP1 targets exhibited a splicing pattern change following treatment with siRNA directed against PTBP1 and PTBP2 in accordance with PTBP1's predicted effect (Fig. 2C; Supplemental Fig. S4A), shifting splicing patterns to those observed in normal colon samples, and two in the opposite direction (Fig. 2D; Supplemental Fig. S4B). A validation of PTBP1 and PTBP2 protein levels upon siRNA treatment demonstrated they were indeed highly reduced (Fig. 2E).

The tested alternative splicing changes in the *RAC1*, *NUMB*, and *PKM* genes were shown to affect protein levels or functions and play an important part in tumorigenesis (see Discussion) (Radisky et al. 2005; Christofk et al. 2008; Misquitta-Ali et al. 2010; Bechara et al. 2013; Myant et al. 2013). Other events are not specifically known to be involved in cancer development but are located within genes that are: *TPM1*, *DNMT3B*, *NCOR2* (also known as *SMRT*), and *SLK* (Jin et al. 2009; Roovers et al. 2009; Choi et al. 2012; Margalef et al. 2012). As the total number of nucleotides in some of these alternative segments is not a multiple of three, their respective addition or deletion from the mRNA is likely to cause a premature stop codon, which could lead to the formation of a truncated protein or to mRNA degradation via nonsense-mediated mRNA decay (NMD). PTBP1 therefore induces splicing pattern changes implicated in cancer development in addition to its interactions with CLIP-derived targets (Fig. 2F). Furthermore, our results demonstrate the utility of our method in identifying proteins that regulate cancerous alternative splicing changes.

ELK1 overexpression activates a regulatory pathway that involves MYC and PTBP1

By focusing on the discovered regulatory pathway involving ELK1, MYC, and PTBP1, we wished to study its induction in a colon tumor–derived cell line. By use of HCT116 cells, the binding of ELK1 to the *MYC* and *PTBP1* promoter regions (Fig. 3A,B), as well as that of MYC to the *PTBP1* promoter region (Fig. 3C), was confirmed via ChIP followed by quantitative real-time-PCR (qPCR; one-sided Student's t-test; $P = 0.002$, $P = 0.001$, and $P =$
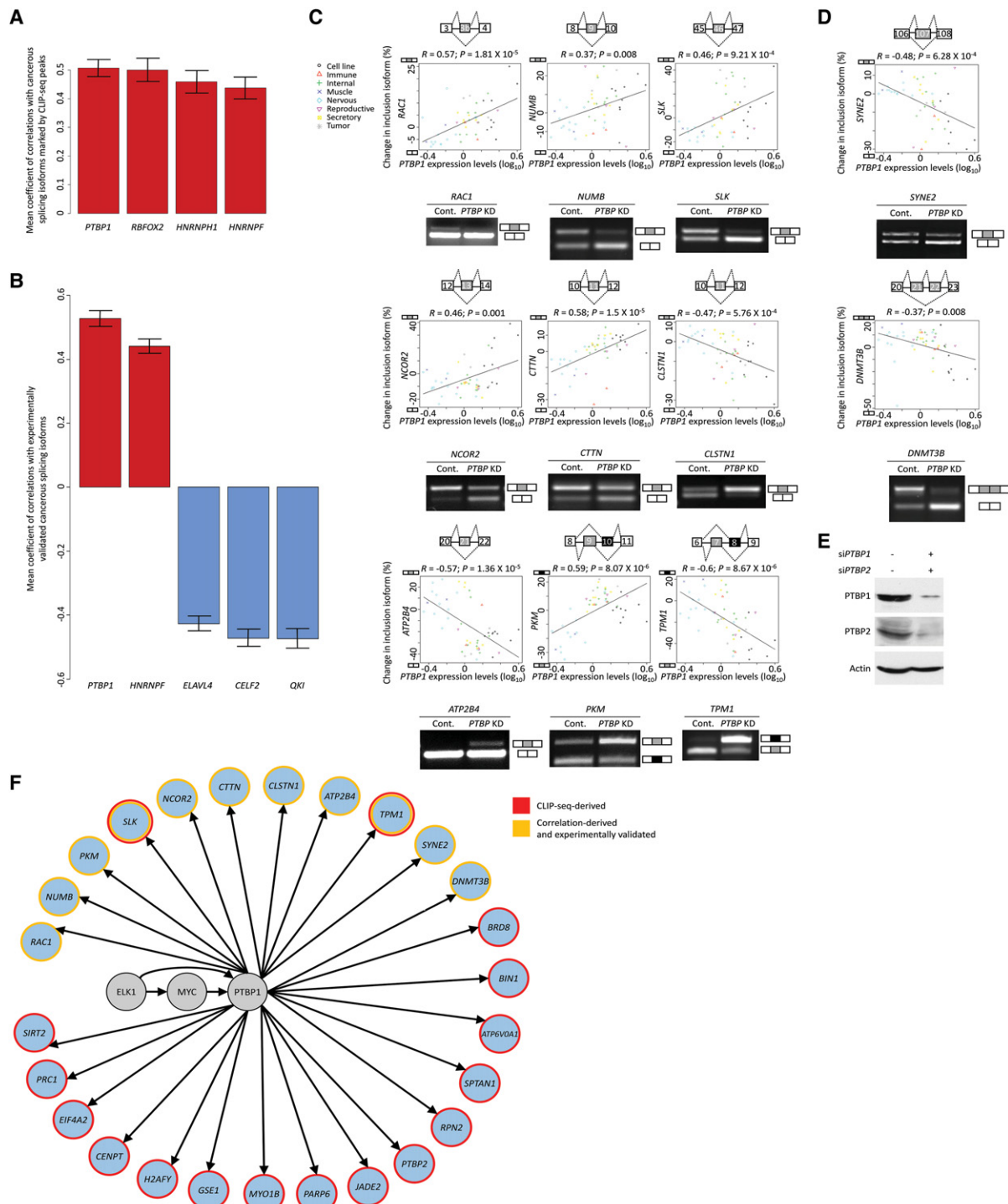
Figure 2. PTBP1 promotes colon tumorigenesis-triggering splicing isoforms. (*A*) Mean Pearson coefficients of ELK1 subnetwork alternative splicing factor gene expression correlations with splicing changes of all cancerous isoforms bound by these factors. Genes displaying fewer than five statistically significant correlations were omitted. Error bars, SEM. (*B*) The five highest ranking mean Pearson coefficients of alternative splicing factor gene expression correlations with the splicing changes of experimentally validated cancerous splicing isoforms. Error bars, SEM. (*C,D, top*) Per each alternative splicing event predicted to be regulated by PTBP1, the Pearson correlation between *PTBP1* gene expression and the change in inclusion splice form across 48 human tissues and cell lines is depicted. Tissue and cell line groups are represented by different symbols. Each diagram depicts exon positions and the possible transcripts arising from the alternative splicing event. (*Bottom*) RT-PCR analysis of the alternative splicing event in HCT116 cells treated with either control siRNA (Cont.) or siRNA directed against *PTBP1* and *PTBP2* (*PTBP* KD) is presented as well. *PKM* and *TPM1* RT-PCR products were digested with PstI. (*E*) HCT116 cells were transfected with control siRNA or siRNA directed against *PTBP1* (si*PTBP1*) and *PTBP2* (si*PTBP2*), and later cell extracts were subjected to Western blot analysis with the indicated antibodies. (*F*) Pathway connecting ELK1 with genes including PTBP1-affected and PTBP1-bound exons exhibiting splicing pattern changes in the colon tumor compared with the normal colon (genes colored light blue; other proteins are colored gray). Genes including exons derived from the analysis in *B* and validated in *C* and *D* are marked by yellow borders. Genes including PTBP1-bound exons are marked by red borders.
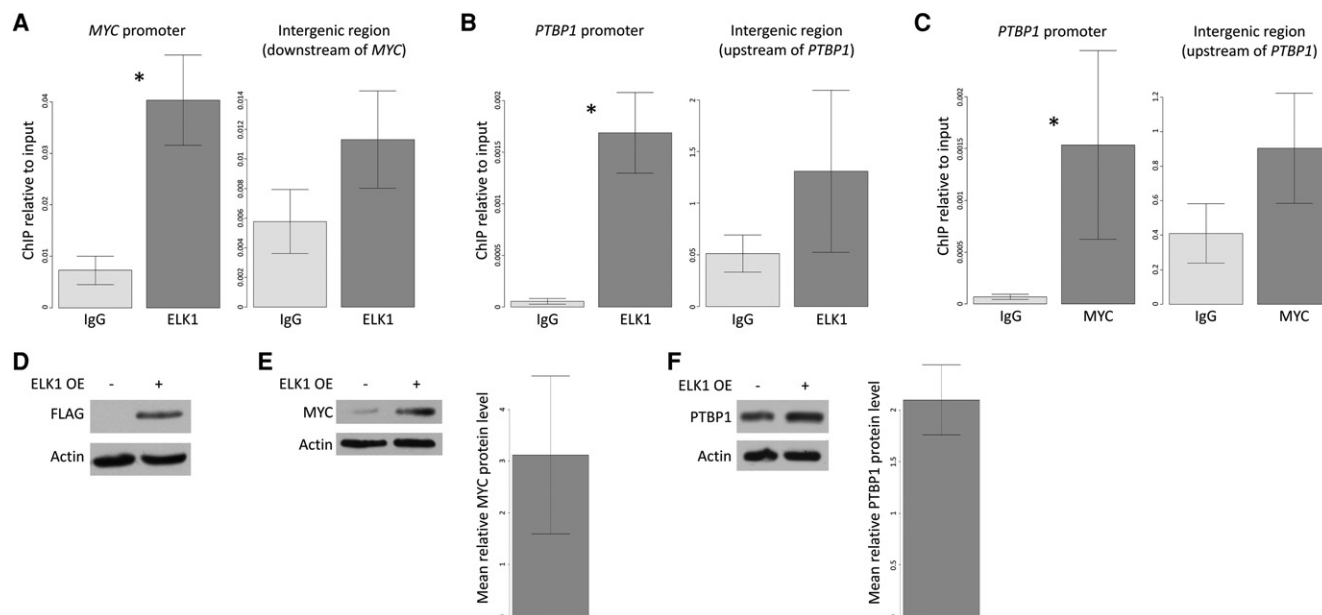
Figure 3. ELK1 activates a regulatory pathway that involves MYC and PTBP1. (*A–C*) HCT116 cells were subjected to ChIP with antibodies against ELK1 (*A,B*) or MYC (*C*). Immunoprecipitated DNA was quantified by qPCR with primers specific to the *MYC* (*A*) and *PTBP1* (*B,C*) promoter regions as well as intergenic regions used as negative controls (Supplemental Methods). Bars, mean values of four (*A,B*) or five (*C*) independent experiments normalized to input (Supplemental Methods). Error bars, SEM. Asterisks indicate $P = 0.002$, $P = 0.001$, and $P = 0.004$, respectively; one-sided Student's *t*-test. (*D–F*) HCT116 cells were transfected with a plasmid containing cDNA encoding *ELK1* (ELK1 OE) or an empty vector in three independent experiments. Cell extracts were subjected to Western blot analysis with the indicated antibodies. Relative protein levels were quantified using ImageJ (Schneider et al. 2012). Error bars, SEM.

0.004, respectively). Additionally, to examine downstream effects on MYC and PTBP1 upon ELK1 level modulation, HCT116 cells were transfected with a plasmid containing cDNA encoding *ELK1*. Upon ELK1 overexpression (Fig. 3D), endogenous MYC and PTBP1 protein levels were 3.12-fold and 2.1-fold higher on average, respectively, than in cells expressing normal levels of *ELK1* (Fig. 3E,F; Supplemental Fig. S4C,D). This demonstrates that ELK1 positively affects the level of these proteins. Several alternative splicing events shown to be affected by *PTBP1* knockdown (Fig. 2C) did not display a splicing pattern change in the majority of independent ELK1 overexpression experiments (data not shown). We hypothesize PTBP1 binding to these RNA targets may be saturated before the increase in endogenous PTBP1 levels that results from ELK1 overexpression. Additionally, analysis of PTBP1-regualted alternative splicing events in the normal colon epithelium cell lines CCD 841 CoN and FHC confirmed that the splicing differences observed between colon tumor and normal colon are indeed cancer associated and do not result from an epithelial-specific splicing program in the tumor, which includes a higher concentration of epithelial cells (Supplemental Fig. S5; Supplemental Results). Overall, our findings demonstrate the activation of the ELK1-induced pathway in a colon cancer cell line.

ELKI, MYC, and *PTBPI* are overexpressed in colon tumors compared with matched normal colon samples

In order to inspect the identified pathway in vivo, we examined the expression patterns of its genes in colon adenocarcinoma samples compared with matched normal tissue samples obtained from 19 patients (Supplemental Table S2). *ELK1*, *MYC*, and *PTBP1* gene expression levels were measured via qRT-PCR. Interestingly, *ELK1* and *PTBP1* were overexpressed in 13 of 19 (68%) patients. In 10 of these 13 patients, *MYC* was overexpressed as well as in an addition-

al three (Methods). One patient displayed extremely high *ELK1*, *MYC*, and *PTBP1* expression levels and was therefore discarded from further qRT-PCR analyses. In the remaining 12 patients, *ELK1*, *MYC*, and *PTBP1* gene expression levels were, respectively, 5.4-fold, 3.36-fold, and 3.53-fold higher in colon tumors than in their matching normal tissues (one-sided Student's *t*-test; $P = 0.02$, $P = 0.04$, and $P = 0.01$, respectively) (Fig. 4A). Moreover, as controls, *AQP8* and *ETS1* gene expression levels were measured (Fig. 4B). Colon tumors were previously shown to express lower levels of *AQP8* in comparison with the normal colon (Gardina et al. 2006), and 16 patients indeed displayed lower levels by 25-fold ($P = 0.01$). ETS1 was connected to the ELK1 subnetwork via a protein–protein interaction, while its gene was not overexpressed in colon tumors (Fig. 1B,C). Our analysis showed that *ETS1* gene expression does not significantly differ between colon tumor samples and normal tissue samples ($P = 0.16$). The splicing patterns of PTBP1-regulated alternative events in the normal and tumor samples were similar to those observed in previous analyses of patient samples (Thorsen et al. 2008; Langer et al. 2010; Misquitta-Ali et al. 2010), as well as in Figure 2, C and D, and Supplemental Fig. S4, A and B (Supplemental Fig. S6).

To assess the pathway in a broader context of colon cancer patients, we examined colon and rectal tumor data derived from the Cancer Genome Atlas (Methods) (The Cancer Genome Research Atlas Network 2012b). Notably, *ELK1*, *MYC*, and *PTBP1* expression profiles in 222 tumors were significantly correlated (Fig. 4C), further validating our identified pathway. Interestingly, *ELK1* displayed a stronger relation with *PTBP1* ($R = 0.47$; $P = 2.36 \times 10^{-13}$) than that between *MYC* and *PTBP1* ($R = 0.27$; $P = 4.16 \times 10^{-5}$), providing additional evidence that ELK1 could play an important role in *PTBP1* transcriptional induction in colon cancer. The relation between *ELK1* and *MYC* ($R = 0.21$; $P = 0.002$) strengthens our previously described results implying that ELK1 serves as an activator of
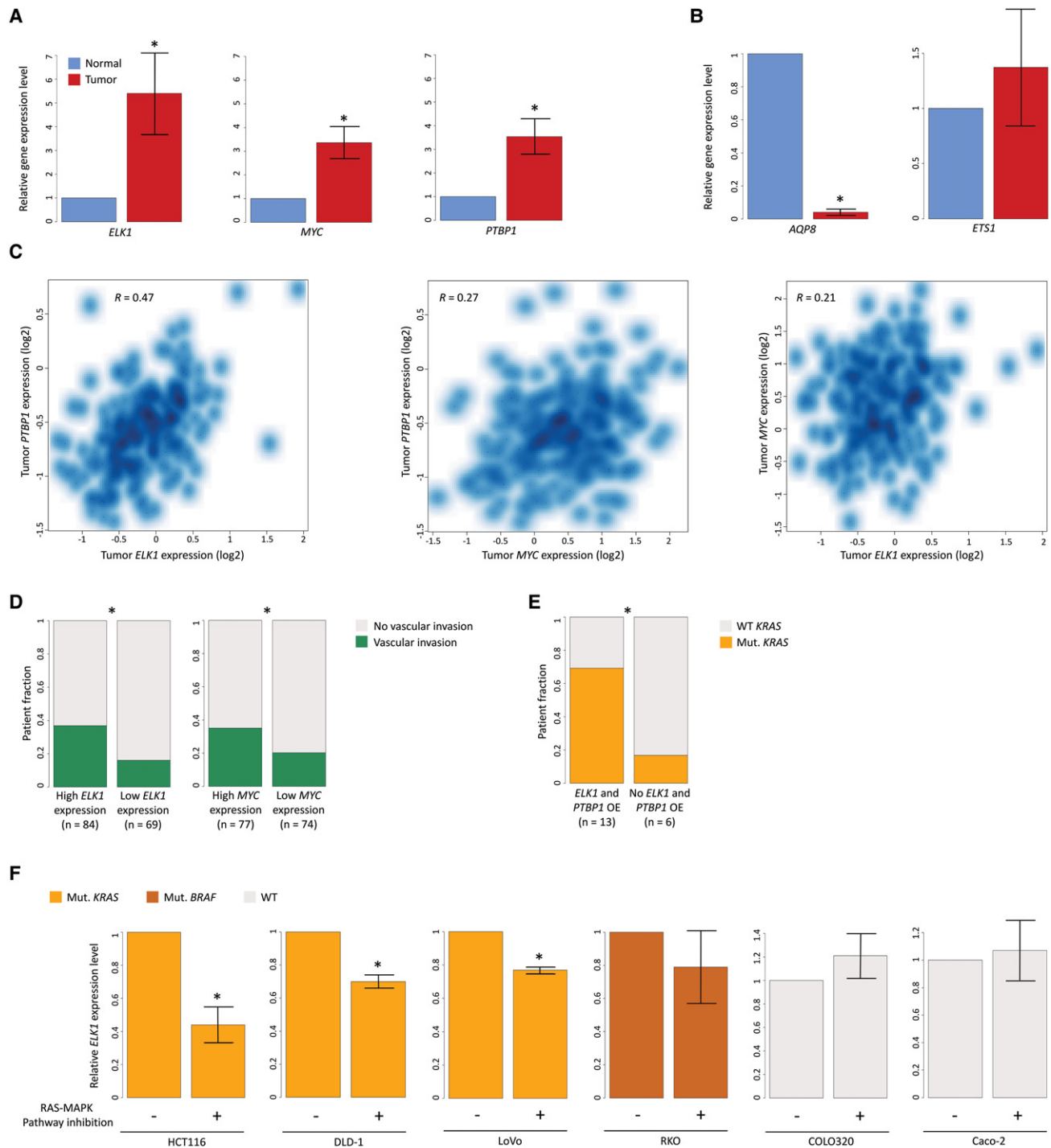
Figure 4. *ELK1*, *MYC*, and *PTBP1* overexpression in colon tumors compared with matched normal colons results from *KRAS* activating mutations. (*A,B*) Total RNA was isolated from colon adenocarcinoma and matched normal colon samples and analyzed by qRT-PCR. (*A*) Mean gene expression levels of *ELK1*, *MYC*, and *PTBP1* in tumors relative to their matched normal tissues in patients exhibiting tumor overexpression of *ELK1* and *PTBP1* ($n = 12$). Asterisks indicate $P = 0.02$, $P = 0.04$, and $P = 0.01$, respectively; one-sided Student's *t*-test. (*B*) As in *A*, but of *AQP8* and *ETS1* in patients exhibiting *AQP8* tumor underexpression ($n = 15$). All values were normalized to *HPRT1* and *GAPDH* in the same sample. Error bars, SEM. (*C*) Smoothed color density representation of the Pearson correlations between the expression levels ($\log_2$) of *ELK1* against *PTBP1* (*left*), *MYC* against *PTBP1* (*middle*), and *ELK1* against *MYC* (*right*) in 222 colorectal tumor samples. (*D*) Fraction of patients bearing tumor vascular invasions among those displaying high *ELK1* (*left*) and *MYC* (*right*) expression levels and among those exhibiting low *ELK1* and *MYC* expression levels. Asterisks indicate $P = 0.003$ and $P = 0.03$, respectively; one-sided Fisher's exact test. (*E*) Fraction of patients bearing *KRAS* mutations (Mut.) among those overexpressing (OE) *ELK1* and *PTBP1* in tumors compared with normal tissues (in *A*) and among those that do not. Asterisk indicates $P = 0.05$; one-sided Fisher's exact test. (*F*) HCT116, DLD-1, LoVo, RKO, COLO320, and Caco-2 cells were treated with U0126 for 24 h, and total RNA was isolated. Bars, mean *ELK1* gene expression levels measured by qRT-PCR in three independent experiments. Values were normalized to *GAPDH* levels in the same experiments. Error bars, SEM. Asterisks indicate $P = 0.03$, $P = 0.01$, and $P = 0.01$, respectively; one-sided Student's *t*-test.

MYC in colon cancer. Examination of Cancer Genome Atlas gene expression data derived from additional cancers (The Cancer Genome Research Atlas Network 2008, 2011, 2012a,c, 2013a) revealed similar correlations in acute myeloid leukemia and clear cell renal cell carcinoma, suggesting the pathway may be active in these cancers as well (Supplemental Fig. S7). We also studied whether a connection exists between our identified pathway and tumor vascular invasion, a predictor of a poor colon cancer prognosis (Lim et al. 2010). Tumors exhibiting high *ELK1* and *MYC* expression levels developed more vascular invasions compared with tumors expressing low levels of these genes (one-sided Fisher's exact test, $P = 0.003$ and $P = 0.03$, respectively) (Fig. 4D). This finding corroborates our results demonstrating the positive effect these two proteins have on PTBP1 expression and the latter's promotion of splicing isoforms that lead to increased cell proliferation and tumor invasiveness. Overall, our findings indicate that the identified colon cancer–associated pathway is active in vivo, testifying to the utility of our network construction method.

KRAS-hyperactivating mutations lead to *ELK1* overexpression in tumors through the activity of the RAS-MAPK pathway

We hypothesized that the underlying cause of *ELK1* overexpression could be the activation of the RAS-MAPK signaling cascade in colon cancer, as *ELK1* is a downstream target of KRAS via this pathway (Lee et al. 2010) and *KRAS* activating mutations were reported in 40%–55% of colon cancer patients (Wood et al. 2007; Fearon 2011; The Cancer Genome Research Atlas Network 2012b). To eliminate other plausible causes, we scanned the COSMIC database (Forbes et al. 2011) and Cancer Genome Atlas data (The Cancer Genome Research Atlas Network 2012b) for *ELK1* mutations or copy number variations in colon and rectal tumors, and indeed, none were observed. Next we scanned the 19 tumor and matched normal tissue samples we had obtained for *KRAS* mutations (Methods) (Supplemental Table S3). Interestingly, tumors overexpressing *ELK1* and *PTBP1* compared with matched normal tissues harbored significantly more *KRAS* activating mutations (Wood et al. 2007; The Cancer Genome Research Atlas Network 2012b) than did tumors that do not exhibit *ELK1* and

PTBP1 overexpression (one-sided Fisher's exact test, $P = 0.05$) (Fig. 4E), suggesting that *ELK1* overexpression in colon tumors results from the activity of the mutant KRAS protein.

To test whether it is the mutant KRAS protein that specifically causes ELK1 overexpression through the RAS-MAPK pathway, we inhibited the pathway's activity by treatment with U0126 (Fournier et al. 2011) and subsequently examined *ELK1* expression levels via qRT-PCR in several colon cancer cell lines: HCT116, DLD-1, and LoVo, which harbor a hyperactivating *KRAS* mutation; RKO, which harbors a hyperactivating *BRAF* mutation that also leads to increased activity of the RAS-MAPK pathway; and COLO320 and Caco-2, which lack mutations leading to increased activity of the RAS-MAPK pathway (Ahmed et al. 2013). A statistically significant decrease in *ELK1* expression levels was observed in all three of the cell lines with mutant *KRAS* (one-sided Student's *t*-test, $P = 0.03$, $P = 0.01$, and $P = 0.01$, respectively) (Fig. 4F) and in none of the cell lines with wild-type *KRAS*. This demonstrates that *ELK1* transcription is induced by the mutant *KRAS* through the RAS-MAPK pathway. Thus, our findings illuminate, for the first time, a full regulatory pathway originating from prevalent cancerous mutations in the colon and leading to functional splicing aberrations that induce tumor formation.

Discussion

Our construction of the colon cancer splicing interactome uncovered a previously unidentified carcinogenesis-favoring regulatory pathway originating in the transcription factor ELK1 (schematically depicted in Fig. 5). This is plausibly due to increased activity of the RAS-MAPK pathway, resulting from oncogenic *KRAS* mutations found in 40%–55% of colon cancer patients (Wood et al. 2007; Fearon 2011; The Cancer Genome Research Atlas Network 2012b). ELK1 has not been previously implicated in colon tumorigenesis but was identified in breast and lung cancer–associated regulatory pathways (Wood et al. 2007; Goodarzi et al. 2009; Lee et al. 2010). The MYC-independent *PTBP1* transcriptional induction could specifically be of therapeutic importance as it presumably contributes to cancer formation without direct MYC involvement, while some potential colon cancer therapy strategies
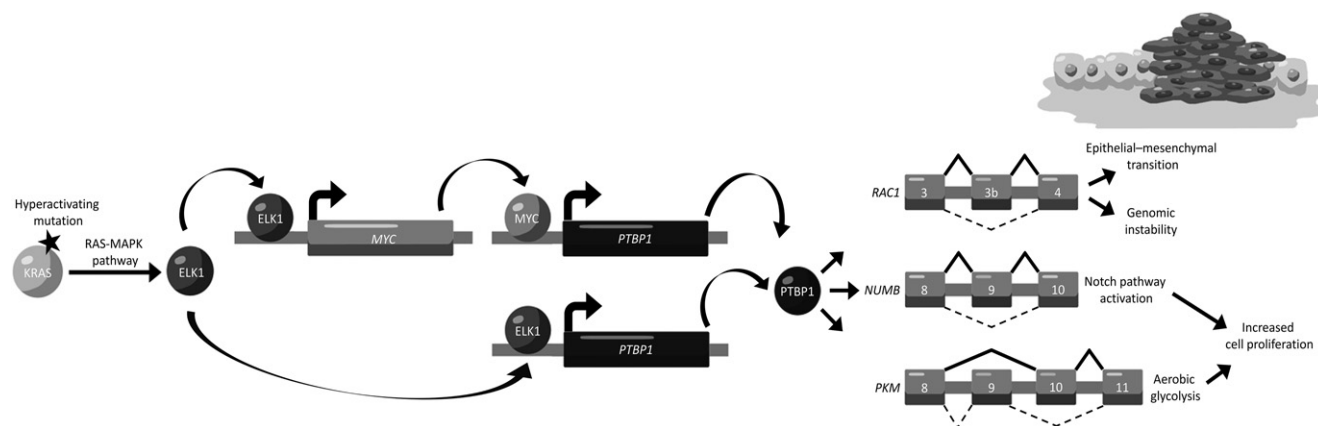

Figure 5. Regulatory pathway leading to colon cancer–promoting splicing aberrations. ELK1 overexpression results from increased activity of the RAS-MAPK pathway due to hyperactivating *KRAS* mutations. This leads to increased transcription of *MYC* and *PTBP1*. Increased MYC levels also lead to increased *PTBP1* levels. PTBP1 overexpression is one of the elements responsible for an alternative splicing profile associated with colon cancer. Among some of the alternative splicing pattern shifts induced by PTBP1 are the inclusion of *RAC1* exon 3b, the increased inclusion of *NUMB* exon 9, and the favoring of *PKM* exon 10 inclusion over exon 9 inclusion. These contribute to colon adenocarcinoma development by increasing cell proliferation and leading to genomic instability and epithelial–mesenchymal transition.

have focused on inhibiting MYC overactivation (Doudican et al. 2014; Zhang et al. 2014).

Colon adenocarcinoma *MYC* expression is mainly up-regulated via the beta-catenin-dependent Wnt signaling pathway due to *APC* mutations in ~70%–80% of patients (Fearon 2011). Our results indicate toward the transcriptional induction of *MYC* by ELK1 in an APC-independent fashion. This is in accordance with evidence of *MYC* up-regulation via the RAS-MAPK pathway in other cancer types (Dang 2012). Further supporting our results, the cancerous RAC1 isoform, which we found to be promoted by PTBP1, was shown to drive tumor initiation together with the oncogenic mutant KRAS (Zhou et al. 2013). Subsequently, other MYC target genes besides *PTBP1* that are known to undergo transcriptional changes in cancer could also be affected by *ELK1* elevation. For example, the expression of *HNRNPA1* and *HNRNPA2B1*, alternative splicing factors that are positively regulated by MYC (Clower et al. 2010; David et al. 2010), could also be influenced by ELK1 up-regulation in colon tumors.

The cancerous splicing changes, which we have revealed to be induced by the regulatory pathway emanating from ELK1, have been shown to significantly contribute to colon cancer development (Fig. 5). For example, the protein resulting from the cancerous inclusion of *RAC1* exon 3b is constitutively active and promotes tumor transformation (Singh et al. 2004). It was shown to increase reactive oxygen species (ROSs), which stimulate epithelial–mesenchymal transition, and cause oxidative damage to DNA and genomic instability (Radisky et al. 2005). Active RAC1 was also identified as a critical protein required for intestinal hyperproliferation (Myant et al. 2013). Additionally, increased inclusion of *NUMB* exon 9 leads to a reduction in NUMB protein levels (Misquitta-Ali et al. 2010). Since NUMB suppresses the Notch signaling pathway (Westhoff et al. 2009), its reduction increases Notch pathway activity and promotes cell proliferation and tumor formation (Misquitta-Ali et al. 2010; Bechara et al. 2013). Finally, *PKM2*, the oncogenic *PKM* isoform that includes exon 10 while lacking exon 9, encodes a protein that shifts cellular metabolism to aerobic glycolysis in the presence of oxygen (the Warburg effect) and promotes tumorigenesis (Christofk et al. 2008). PKM2 also displays other essential nonmetabolic functions in cancer formation such as the regulation of beta-catenin transactivation (Yang et al. 2011), chromosome segregation, and mitosis progression (Jiang et al. 2014).

PTBP1 and PTBP2 negatively regulate each other's levels by affecting the splicing pattern of their pre-mRNAs, and their genes are mainly expressed in different tissues (Boutz et al. 2007; Spellman et al. 2007). While *PTBP1* expression is generally low in the nervous system and its transcriptional down-regulation plays an important part in neuronal differentiation (Xue et al. 2013), *PTBP2* is mainly expressed in the nervous system (Boutz et al. 2007; Li et al. 2014). In agreement with our results in Figure 2 demonstrating the effect PTBP1 has in promoting colon tumorigenesis-triggering splicing isoforms, *PTBP1* knockdown significantly reduces the invasive capacity of a colon cancer cell line, T84, and a prostate cancer cell line, PC-3M (Wang et al. 2008a). In this study, *PTBP1* knockdown in HeLa cells resulted in the opposite effect. Since PTBP2 expression level elevates in HeLa cells upon *PTBP1* knockdown (Spellman et al. 2007; Llorian et al. 2010), we speculate the observed phenomenon in these cells may be due to PTBP2 compensation upon PTBP1 reduction.

Examination of data obtained from the Cancer Genome Atlas for *ELK1*, *MYC*, and *PTBP1* expression in cancer samples suggests the identified interactions between them could be active in acute myeloid leukemia and clear cell renal cell carcinoma as well (Supplemental Fig. S7). Our results also suggest ELK1 may strongly affect *PTBP1* induction in breast cancer, and are in agreement with previous evidence of positive regulation of *PTBP1* by MYC in glioblastoma and lung cancer (Chen et al. 2010; Clower et al. 2010; David et al. 2010). Additionally, the enrichment of our discovered lung cancer subnetworks for KEGG cancerous pathways and COSMIC genes testifies to the general applicability of our network construction method (Supplemental Fig. S2; Supplemental Table S1). It could therefore be applied to transcriptomic data derived from other cancers. It will be of future interest to determine the splicing interactomes of different tumor types and compare between them in order to identify shared pathways and those that are specific to certain cancers. As additional large-scale physical interaction data become publicly available, incorporating these data into our network to provide a more comprehensive overview of significant subnetworks of interest is of importance for future work. Finally, the construction of the cancerous splicing interactome for individual patients based on tissue sample high-throughput RNA sequencing (RNA-seq) data would allow patient comparison and could lead to new insights pertaining to tumor classification and patient prognosis as well as the identification of potential therapeutic targets.

Methods

Network-based inference of cancerous alternative splicing regulation

We integrated heterogeneous data into a single network of physical interactions. Specifically, 16,320 protein–DNA interactions connecting 32 transcription factors with the genes they bind and data pertaining to 45,055 protein–protein interactions were derived from publicly available data (Yosef et al. 2011; Hegele et al. 2012). To connect alternative splicing factors with the alternative splicing events they bind, we first annotated all nonoverlapping internal human exons included in multiexonic genes. Annotations were derived from hg18 RefSeq genes, downloaded from the UCSC Genome Browser (Rhead et al. 2010). Then, high-throughput CLIP tag peaks (HITS-CLIP/CLIP-seq, PAR-CLIP, and iCLIP) (Sanford et al. 2009; Xiao et al. 2009; Xue et al. 2009; Yeo et al. 2009; Hafner et al. 2010; Konig et al. 2010; Wang et al. 2010; Kishore et al. 2011; Lebedeva et al. 2011; Mukherjee et al. 2011; Tollervey et al. 2011; Huelga et al. 2012) were detected as previously specified (Hafner et al. 2010; Kishore et al. 2011; Huelga et al. 2012). Finally, the top 5% scoring peaks overlapping with a window located 300 bp upstream of the annotated exons to 300 bp downstream from them, accounting for 15,501 protein–RNA interactions and 23,527 alternative splicing events, were integrated into the network. The combined network is available at http://www.cs.tau.ac.il/~bnet/ANAT.

Previously, we described an approach to infer a subnetwork connecting a set of causal proteins with a set of affected proteins (Yosef et al. 2009, 2011). Here, we build upon this approach to connect transcription factors with differentially spliced exons in tumors. Specifically, we retrieved transcriptome-wide microarray data in 48 human tissues, tumors, and cancer cell lines from Castle et al. (2008) and analyzed them to determine the alternative splicing and gene expression tissue profiles of 24,426 alternative splicing events and 18,093 genes (as specified there). Exon annotations in our physical interaction network were merged with those of the alternative splicing events covered by the data of Castle et al. (2008). Alternative splicing events were considered differentially spliced in tumors compared with the normal tissue if they

displayed a significant splicing change in the tumor compared with a mixed tissue pool while not in the normal tissue compared with a mixed tissue pool, or if both tissue types did and their splicing isoform change difference was ≥20%. Each subnetwork, connecting a transcription factor to the events that are alternatively spliced in tumors, was then scored according to the gene expression changes it spans (sum of subnetwork absolute gene expression level differences between the tumor and the normal tissue, excluding subnetwork genes included in it only due to protein–RNA interactions), normalized by its size (number of nodes). These scores were compared with the scores of 100 subnetworks connecting the same transcription factor with random alternative splicing events (random alternative splicing event sets were of the same size as the test set). We only considered significant results with empirical P-values lower than 0.1 (for the ELK1 subnetwork, $P = 0.09$). Finally, we computed the FDR-corrected P-values of hypergeometric intersections between the significant subnetworks and either the union of cancer-associated KEGG pathways (Kanehisa et al. 2012) or mutated genes in cancer derived from COSMIC (Supplemental Table S1; Forbes et al. 2011). ANAT source code is available at https://bitbucket.org/rinatias/anat/branch/OpenSource, and subnetwork analysis and scoring scripts are included as supplemental files.

ChIP-seq analysis

ELK1, MYC, and input ChIP-seq data were downloaded from the GEO (GSM935326, GSM935320, GSM935339, and GSM817342). Data were aligned to the hg18 human genome assembly using Bowtie (Langmead et al. 2009) while allowing for one mismatch per read, and only uniquely mapped reads were used for further processing. In order to allow compatibility between the various data sets used in our study, NGS reads were not mapped to the most recent human genome assembly (GCRh38). However, it should be noted that only very minor differences, if any, exist between the sequences of the coding regions of the genome in different genome assemblies. Since all the analyses we performed focused solely on genes and mainly at an exon-centric resolution, it is very unlikely that remapping the data to a more recent assembly of the human genome would have any effect on our results, as the vast majority of reads, if not all of them, would align to exactly the same areas in the genome. ChIP-seq peak calling and annotation analyses were carried out using HOMER (Heinz et al. 2010) against input ChIP-seq data as controls. HOMER default definition of promoters as regions spanning −1 kb to +100 bp of transcription start sites was used.

In silico identification of colon cancer alternative splicing regulators

The Pearson correlations between the splicing profiles of 54 cancer-associated alternative splicing events (Jordan et al. 1999; Hardt et al. 2003; Ghigna et al. 2005; Gardina et al. 2006; Klinck et al. 2008; Thorsen et al. 2008; Venables et al. 2009; Langer et al. 2010; Misquitta-Ali et al. 2010; Pio et al. 2010; Choi et al. 2011; Ishimoto et al. 2011; Liu et al. 2012; Miura et al. 2012; Seo et al. 2012) across all tissues and the gene expression profiles of alternative splicing factors (gene list derived from Chen and Manley 2009 and Hegele et al. 2012) in the same tissues were computed (alternative splicing and gene expression data were derived from Castle et al. 2008). Alternative splicing factor genes not displaying a significant expression level change in colon tumors compared with a mixed tissue pool were discarded as were splicing events with significant isoform changes compared with a mixed tissue pool in only four tissues or less, and statistically insignificant cor-

relations ($P > 0.05$). Genes were ranked according to the number of their statistically significant correlations and the mean absolute correlation coefficient values.

TCGA data analysis

Human colon and rectal cancer gene expression data and tumor characteristics (The Cancer Genome Research Atlas Network 2012b) as well as acute myeloid leukemia (The Cancer Genome Research Atlas Network 2013b), clear cell renal cell carcinoma (The Cancer Genome Research Atlas Network 2013a), breast cancer (The Cancer Genome Research Atlas Network 2012c), squamous cell lung cancer (The Cancer Genome Research Atlas Network 2012a), glioblastoma (The Cancer Genome Research Atlas Network 2008), and ovarian cancer (The Cancer Genome Research Atlas Network 2011) gene expression data were downloaded from the Cancer Genome Atlas portal (http://cancergenome.nih.gov/). Colorectal tumors were divided to three equally sized bins according to *ELK1* or *MYC* expression. Per each gene expression profile, tumors included in the top bin were defined as displaying high expression, while those included in the bottom bin were defined as exhibiting low expression.

Cell culture, cloning, and transfection

HCT116, DLD-1, LoVo, COLO320, and Caco-2 cells were cultured in RPMI1640. RKO cells were cultured in DMEM. Media were supplemented with 0.29 mg/mL L-glutamine, 100 U/mL penicillin, and 0.1 mg/mL streptomycin (Biological Industries) and 10% fetal calf serum (Sigma) in 37°C humidified atmosphere with 5% CO_2. Upon testing, cells were found to be free of mycoplasma contamination. Human *PTBP1* and *ELK1* coding sequences were amplified by KAPA HiFi HotStart (Kapa Biosystems) and cloned into pX3FLAG-CMV-10 expression vector. HCT116 cells were plated in six-well plates for 24 h prior to transfection of 500 ng of each vector using TransIT-LT1 reagent (Mirus) and were harvested after 48 h. SiRNA transfection of HCT116 cells was carried out using Lipofectamine RNAiMAX (Invitrogen) according to the manufacturer's protocol with 100 pmol of each of the siPTBP1 and siPTBP2 and with 200 pmol of the control siGENOME nontargeting human siRNA pool 2 (all purchased from Dharmacon). Cells were harvested 48 h after transfection. siRNA sequences are as follows: siPTBP1, 5′-CUUCCAUCAUUCCAGAGAAUU-3′; si-PTBP2, 5′-GAGAGGAUCUGACGAACUAUU-3′ (derived from Llorian et al. 2010). HCT116, DLD-1, LoVo, COLO320, and Caco-2 cells were treated with U0126 (Calbiochem) for RAS-MAPK pathway inhibition and were harvested after 24 h; untreated cells were used as a control. Cell pellets from all experiments were divided to RNA and protein purification.

Colon adenocarcinoma and normal colon samples

Fresh-frozen (FF) tissue samples, both tumor and tumor-free (normal), from 19 colon adenocarcinoma patients (Supplemental Table S2) were obtained from the Institutional Tissue Banks at Sheba Medical Center following IRB approval and consent of patients.

RNA purification, RT-PCR, quantitative RT-PCR, and *KRAS* sequencing

RNA was extracted from cell lines with TRI reagent (Sigma). Total RNA was also isolated from human colon tumor samples and their matched normal tissue samples. Tissue samples were mechanically homogenized, and RNA was obtained using TRI reagent (Sigma), according to the manufacturer's protocol. After DNase I digestion

(Ambion), 2 µg total RNA was reverse transcribed by SuperScript III (Invitrogen).

Splicing products were amplified with red load Taq master mix (Larova) or bio-ready mix (Biolab) and separated on 1.5% agarose gel. In the cases of *TPM1* and *PKM* alternative splicing events, PCR products were digested by PstI enzyme (New England BioLabs) prior to separation in 2% agarose gel. A qPCR analysis of mRNA expression in human tissue samples and cell lines was conducted using KAPA SYBR fast qPCR master mix (Kapa Biosystems) in a StepOne plus thermocycler PCR machine (Applied Biosystems) according to the manufacturer's instructions. Expression levels of *HPRT1* and *GAPDH* genes were used as endogenous controls, and all of the samples were assayed in triplicate. Genes demonstrating an expression level increase of >10% in each tumor sample in comparison with the matched normal sample were considered overexpressed for further statistical analyses. The log base 2 of all values were computed to meet the assumptions of the statistical tests. Variance similarity between examined groups was tested using an *F*-test, and in all cases, the variances were found to be different and treated as such in further statistical tests.

Known (Wood et al. 2007; The Cancer Genome Research Atlas Network 2012b) and novel colon cancer *KRAS* mutations were examined in tumor samples in comparison with their matched normal samples by Sanger sequencing following cDNA amplification.

Data access

Sanger sequencing data from this study have been submitted to the NCBI Trace Archive (http://www.ncbi.nlm.nih.gov/Traces/home/) under TI numbers 2343078499–2343078575.

Acknowledgments

References

Adler AS, McCleland ML, Yee S, Yaylaoglu M, Hussain S, Cosino E, Quinones G, Modrusan Z, Seshagiri S, Torres E, et al. 2014. An integrative analysis of colon cancer identifies an essential function for PRPF6 in tumor growth. *Genes Dev* **28:** 1068–1084.

Ahmed D, Eide PW, Eilertsen IA, Danielsen SA, Eknaes M, Hektoen M, Lind GE, Lothe RA. 2013. Epigenetic and genetic features of 24 colon cancer cell lines. *Oncogenesis* **2:** e71.

Balasubramani M, Day BW, Schoen RE, Getzenberg RH. 2006. Altered expression and localization of creatine kinase B, heterogeneous nuclear ribonucleoprotein F, and high mobility group box 1 protein in the nuclear matrix associated with colon cancer. *Cancer Res* **66:** 763–769.

Bechara EG, Sebestyen E, Bernardis I, Eyras E, Valcarcel J. 2013. RBM5, 6, and 10 differentially regulate NUMB alternative splicing to control cancer cell proliferation. *Mol Cell* **52:** 720–733.

Boutz PL, Stoilov P, Li Q, Lin CH, Chawla G, Ostrow K, Shiue L, Ares M Jr, Black DL. 2007. A post-transcriptional regulatory switch in polypyrimidine tract-binding proteins reprograms alternative splicing in developing neurons. *Genes Dev* **21:** 1636–1652.

The Cancer Genome Research Atlas Network. 2008. Comprehensive genomic characterization defines human glioblastoma genes and core pathways. *Nature* **455:** 1061–1068.

The Cancer Genome Research Atlas Network. 2011. Integrated genomic analyses of ovarian carcinoma. *Nature* **474:** 609–615.

The Cancer Genome Research Atlas Network. 2012a. Comprehensive genomic characterization of squamous cell lung cancers. *Nature* **489:** 519–525.

The Cancer Genome Research Atlas Network. 2012b. Comprehensive molecular characterization of human colon and rectal cancer. *Nature* **487:** 330–337.

The Cancer Genome Research Atlas Network. 2012c. Comprehensive molecular portraits of human breast tumours. *Nature* **490:** 61–70.

The Cancer Genome Research Atlas Network. 2013a. Comprehensive molecular characterization of clear cell renal cell carcinoma. *Nature* **499:** 43–49.

The Cancer Genome Research Atlas Network. 2013b. Genomic and epigenomic landscapes of adult de novo acute myeloid leukemia. *N Engl J Med* **368:** 2059–2074.

Castle JC, Zhang C, Shah JK, Kulkarni AV, Kalsotra A, Cooper TA, Johnson JM. 2008. Expression of 24,426 human alternative splicing events and predicted *cis* regulation in 48 tissues and cell lines. *Nat Genet* **40:** 1416–1425.

Chen M, Manley JL. 2009. Mechanisms of alternative splicing regulation: insights from molecular and genomics approaches. *Nat Rev Mol Cell Biol* **10:** 741–754.

Chen M, Zhang J, Manley JL. 2010. Turning on a fuel switch of cancer: hnRNP proteins regulate alternative splicing of pyruvate kinase mRNA. *Cancer Res* **70:** 8977–8980.

Choi JW, Kim DG, Lee AE, Kim HR, Lee JY, Kwon NH, Shin YK, Hwang SK, Chang SH, Cho MH, et al. 2011. Cancer-associated splicing variant of tumor suppressor AIMP2/p38: pathological implication in tumorigenesis. *PLoS Genet* **7:** e1001351.

Choi C, Kim D, Kim S, Jeong S, Song E, Helfman DM. 2012. From skeletal muscle to cancer: insights learned elucidating the function of tropomyosin. *J Struct Biol* **177:** 63–69.

Christofk HR, Vander Heiden MG, Harris MH, Ramanathan A, Gerszten RE, Wei R, Fleming MD, Schreiber SL, Cantley LC. 2008. The M2 splice isoform of pyruvate kinase is important for cancer metabolism and tumour growth. *Nature* **452:** 230–233.

Clower CV, Chatterjee D, Wang Z, Cantley LC, Vander Heiden MG, Krainer AR. 2010. The alternative splicing repressors hnRNP A1/A2 and PTB influence pyruvate kinase isoform expression and cell metabolism. *Proc Natl Acad Sci* **107:** 1894–1899.

Cohen-Eliav M, Golan-Gerstl R, Siegfried Z, Andersen CL, Thorsen K, Orntoft TF, Mu D, Karni R. 2013. The splicing factor SRSF6 is amplified and is an oncoprotein in lung and colon cancers. *J Pathol* **229:** 630–639.

Cooper TA, Wan L, Dreyfuss G. 2009. RNA and disease. *Cell* **136:** 777–793.

Cunningham D, Atkin W, Lenz HJ, Lynch HT, Minsky B, Nordlinger B, Starling N. 2010. Colorectal cancer. *Lancet* **375:** 1030–1047.

Dang CV. 2012. *MYC* on the path to cancer. *Cell* **149:** 22–35.

Das S, Anczuków O, Akerman M, Krainer AR. 2012. Oncogenic splicing factor *SRSF1* is a critical transcriptional target of MYC. *Cell Rep* **1:** 110–117.

David CJ, Manley JL. 2010. Alternative pre-mRNA splicing regulation in cancer: pathways and programs unhinged. *Genes Dev* **24:** 2343–2364.

David CJ, Chen M, Assanah M, Canoll P, Manley JL. 2010. HnRNP proteins controlled by c-Myc deregulate pyruvate kinase mRNA splicing in cancer. *Nature* **463:** 364–368.

Doudican NA, Mazumder A, Kapoor S, Sultana Z, Kumar A, Talawdekar A, Basu K, Agrawal A, Aggarwal A, Shetty K, et al. 2014. Predictive simulation approach for designing cancer therapeutic regimens with novel biological mechanisms. *J Cancer* **5:** 406–416.

The ENCODE Project Consortium. 2012. An integrated encyclopedia of DNA elements in the human genome. *Nature* **489:** 57–74.

Fearon ER. 2011. Molecular genetics of colorectal cancer. *Annu Rev Pathol* **6:** 479–507.

Forbes SA, Bindal N, Bamford S, Cole C, Kok CY, Beare D, Jia M, Shepherd R, Leung K, Menzies A, et al. 2011. COSMIC: mining complete cancer genomes in the Catalogue of Somatic Mutations in Cancer. *Nucleic Acids Res* **39**(Database issue)**:** D945–D950.

Fournier G, Cabaud O, Josselin E, Chaix A, Adelaide J, Isnardon D, Restouin A, Castellano R, Dubreuil P, Chaffanet M, et al. 2011. Loss of AF6/afadin, a marker of poor outcome in breast cancer, induces cell migration, invasiveness and tumor growth. *Oncogene* **30:** 3862–3874.

Gardina PJ, Clark TA, Shimada B, Staples MK, Yang Q, Veitch J, Schweitzer A, Awad T, Sugnet C, Dee S, et al. 2006. Alternative splicing and differential gene expression in colon cancer detected by a whole genome exon array. *BMC Genomics* **7:** 325.

Ghigna C, Giordano S, Shen H, Benvenuto F, Castiglioni F, Comoglio PM, Green MR, Riva S, Biamonti G. 2005. Cell motility is controlled by SF2/ASF through alternative splicing of the *Ron* protooncogene. *Mol Cell* **20:** 881–890.

Golan-Gerstl R, Cohen M, Shilo A, Suh SS, Bakacs A, Coppola L, Karni R. 2011. Splicing factor hnRNP A2/B1 regulates tumor suppressor gene splicing and is an oncogenic driver in glioblastoma. *Cancer Res* **71:** 4464–4472.

Goodarzi H, Elemento O, Tavazoie S. 2009. Revealing global regulatory perturbations across human cancers. *Mol Cell* **36:** 900–911.

Graubert TA, Shen D, Ding L, Okeyo-Owuor T, Lunn CL, Shao J, Krysiak K, Harris CC, Koboldt DC, Larson DE, et al. 2011. Recurrent mutations in the *U2AF1* splicing factor in myelodysplastic syndromes. *Nat Genet* **44:** 53–57.

Guigo R, Valcarcel J. 2006. Unweaving the meanings of messenger RNA sequences. *Mol Cell* **23:** 150–151.

Hafner M, Landthaler M, Burger L, Khorshid M, Hausser J, Berninger P, Rothballer A, Ascano M Jr, Jungkamp AC, Munschauer M, et al. 2010. Transcriptome-wide identification of RNA-binding protein and microRNA target sites by PAR-CLIP. *Cell* **141:** 129–141.

Hardt PD, Toepler M, Ngoumou B, Rupp J, Kloer HU. 2003. Measurement of fecal pyruvate kinase type M2 (tumor M2-PK) concentrations in patients with gastric cancer, colorectal cancer, colorectal adenomas and controls. *Anticancer Res* **23:** 851–853.

He X, Arslan AD, Ho TT, Yuan C, Stampfer MR, Beck WT. 2014. Involvement of polypyrimidine tract-binding protein (PTBP1) in maintaining breast cancer cell growth and malignant properties. *Oncogenesis* **3:** e84.

Hegele A, Kamburov A, Grossmann A, Sourlis C, Wowro S, Weimann M, Will CL, Pena V, Luhrmann R, Stelzl U. 2012. Dynamic protein-protein interaction wiring of the human spliceosome. *Mol Cell* **45:** 567–580.

Heinz S, Benner C, Spann N, Bertolino E, Lin YC, Laslo P, Cheng JX, Murre C, Singh H, Glass CK. 2010. Simple combinations of lineage-determining transcription factors prime *cis*-regulatory elements required for macrophage and B cell identities. *Mol Cell* **38:** 576–589.

Huelga SC, Vu AQ, Arnold JD, Liang TY, Liu PP, Yan BY, Donohue JP, Shiue L, Hoon S, Brenner S, et al. 2012. Integrative genome-wide analysis reveals cooperative regulation of alternative splicing by hnRNP proteins. *Cell Rep* **1:** 167–178.

Ishimoto T, Nagano O, Yae T, Tamada M, Motohara T, Oshima H, Oshima M, Ikeda T, Asaba R, Yagi H, et al. 2011. CD44 variant regulates redox status in cancer cells by stabilizing the xCT subunit of system xc− and thereby promotes tumor growth. *Cancer Cell* **19:** 387–400.

Jiang Y, Li X, Yang W, Hawke DH, Zheng Y, Xia Y, Aldape K, Wei C, Guo F, Chen Y, et al. 2014. PKM2 regulates chromosome segregation and mitosis progression of tumor cells. *Mol Cell* **53:** 75–87.

Jin B, Yao B, Li JL, Fields CR, Delmas AL, Liu C, Robertson KD. 2009. DNMT1 and DNMT3B modulate distinct polycomb-mediated histone modifications in colon cancer. *Cancer Res* **69:** 7412–7421.

Jordan P, Brazao R, Boavida MG, Gespach C, Chastre E. 1999. Cloning of a novel human Rac1b splice variant with increased expression in colorectal tumors. *Oncogene* **18:** 6835–6839.

Kanehisa M, Goto S, Sato Y, Furumichi M, Tanabe M. 2012. KEGG for integration and interpretation of large-scale molecular data sets. *Nucleic Acids Res* **40**(Database issue)**:** D109–D114.

Karni R, de Stanchina E, Lowe SW, Sinha R, Mu D, Krainer AR. 2007. The gene encoding the splicing factor SF2/ASF is a proto-oncogene. *Nat Struct Mol Biol* **14:** 185–193.

Keppetipola N, Sharma S, Li Q, Black DL. 2012. Neuronal regulation of pre-mRNA splicing by polypyrimidine tract binding proteins, PTBP1 and PTBP2. *Crit Rev Biochem Mol Biol* **47:** 360–378.

Kim E, Goren A, Ast G. 2008. Insights into the connection between cancer and alternative splicing. *Trends Genet* **24:** 7–10.

Kishore S, Jaskiewicz L, Burger L, Hausser J, Khorshid M, Zavolan M. 2011. A quantitative analysis of CLIP methods for identifying binding sites of RNA-binding proteins. *Nat Methods* **8:** 559–564.

Klinck R, Bramard A, Inkel L, Dufresne-Martin G, Gervais-Bird J, Madden R, Paquet ER, Koh C, Venables JP, Prinos P, et al. 2008. Multiple alternative splicing markers for ovarian cancer. *Cancer Res* **68:** 657–663.

Kloetgen A, Munch PC, Borkhardt A, Hoell JI, McHardy AC. 2014. Biochemical and bioinformatic methods for elucidating the role of RNA–protein interactions in posttranscriptional regulation. *Brief Funct Genomics* **14:** 102–114.

Konig J, Zarnack K, Rot G, Curk T, Kayikci M, Zupan B, Turner DJ, Luscombe NM, Ule J. 2010. iCLIP reveals the function of hnRNP particles in splicing at individual nucleotide resolution. *Nat Struct Mol Biol* **17:** 909–915.

Langer W, Sohler F, Leder G, Beckmann G, Seidel H, Grone J, Hummel M, Sommer A. 2010. Exon array analysis using re-defined probe sets results in reliable identification of alternatively spliced genes in non-small cell lung cancer. *BMC Genomics* **11:** 676.

Langmead B, Trapnell C, Pop M, Salzberg SL. 2009. Ultrafast and memory-efficient alignment of short DNA sequences to the human genome. *Genome Biol* **10:** R25.

Lebedeva S, Jens M, Theil K, Schwanhausser B, Selbach M, Landthaler M, Rajewsky N. 2011. Transcriptome-wide analysis of regulatory interactions of the RNA-binding protein HuR. *Mol Cell* **43:** 340–352.

Lee W, Jiang Z, Liu J, Haverty PM, Guan Y, Stinson J, Yue P, Zhang Y, Pant KP, Bhatt D, et al. 2010. The mutation spectrum revealed by paired genome sequences from a lung cancer patient. *Nature* **465:** 473–477.

Li Q, Zheng S, Han A, Lin CH, Stoilov P, Fu XD, Black DL. 2014. The splicing regulator PTBP2 controls a program of embryonic splicing required for neuronal maturation. *eLife* **3:** e01201.

Lim SB, Yu CS, Jang SJ, Kim TW, Kim JH, Kim JC. 2010. Prognostic significance of lymphovascular invasion in sporadic colorectal cancer. *Dis Colon Rectum* **53:** 377–384.

Liu J, Lee W, Jiang Z, Chen Z, Jhunjhunwala S, Haverty PM, Gnad F, Guan Y, Gilbert HN, Stinson J, et al. 2012. Genome and transcriptome sequencing of lung cancers reveal diverse mutational and splicing events. *Genome Res* **22:** 2315–2327.

Llorian M, Schwartz S, Clark TA, Hollander D, Tan LY, Spellman R, Gordon A, Schweitzer AC, de la Grange P, Ast G, et al. 2010. Position-dependent alternative splicing activity revealed by global profiling of alternative splicing events regulated by PTB. *Nat Struct Mol Biol* **17:** 1114–1123.

Mallinjoud P, Villemin JP, Mortada H, Polay Espinoza M, Desmet FO, Samaan S, Chautard E, Tranchevent LC, Auboeuf D. 2014. Endothelial, epithelial, and fibroblast cells exhibit specific splicing programs independently of their tissue of origin. *Genome Res* **24:** 511–521.

Margalef P, Fernandez-Majada V, Villanueva A, Garcia-Carbonell R, Iglesias M, Lopez L, Martinez-Iniesta M, Villa-Freixa J, Mulero MC, Andreu M, et al. 2012. A truncated form of IKKα is responsible for specific nuclear IKK activity in colorectal cancer. *Cell Rep* **2:** 840–854.

Mickleburgh I, Kafasla P, Cherny D, Llorian M, Curry S, Jackson RJ, Smith CW. 2014. The organization of RNA contacts by PTB for regulation of *FAS* splicing. *Nucleic Acids Res* **42:** 8605–8620.

Misquitta-Ali CM, Cheng E, O'Hanlon D, Liu N, McGlade CJ, Tsao MS, Blencowe BJ. 2010. Global profiling and molecular characterization of alternative splicing events misregulated in lung cancer. *Mol Cell Biol* **31:** 138–150.

Miura K, Fujibuchi W, Unno M. 2012. Splice isoforms as therapeutic targets for colorectal cancer. *Carcinogenesis* **33:** 2311–2319.

Mukherjee N, Corcoran DL, Nusbaum JD, Reid DW, Georgiev S, Hafner M, Ascano M Jr, Tuschl T, Ohler U, Keene JD. 2011. Integrative regulatory mapping indicates that the RNA-binding protein HuR couples pre-mRNA processing and mRNA stability. *Mol Cell* **43:** 327–339.

Myant KB, Cammareri P, McGhee EJ, Ridgway RA, Huels DJ, Cordero JB, Schwitalla S, Kalna G, Ogg EL, Athineos D, et al. 2013. ROS production and NF-κB activation triggered by RAC1 facilitate WNT-driven intestinal stem cell proliferation and colorectal cancer initiation. *Cell Stem Cell* **12:** 761–773.

Pan Q, Shai O, Lee LJ, Frey BJ, Blencowe BJ. 2008. Deep surveying of alternative splicing complexity in the human transcriptome by high-throughput sequencing. *Nat Genet* **40:** 1413–1415.

Papasaikas P, Tejedor JR, Vigevani L, Valcarcel J. 2015. Functional splicing network reveals extensive regulatory potential of the core spliceosomal machinery. *Mol Cell* **57:** 7–22.

Pesson M, Volant A, Uguen A, Trillet K, De La Grange P, Aubry M, Daoulas M, Robaszkiewicz M, Le Gac G, Morel A, et al. 2014. A gene expression and pre-mRNA splicing signature that marks the adenoma-adenocarcinoma progression in colorectal cancer. *PLoS One* **9:** e87761.

Pio R, Blanco D, Pajares MJ, Aibar E, Durany O, Ezponda T, Agorreta J, Gomez-Roman J, Anton MA, Rubio A, et al. 2010. Development of a novel splice array platform and its application in the identification of alternative splice variants in lung cancer. *BMC Genomics* **11:** 352.

Quesada V, Conde L, Villamor N, Ordonez GR, Jares P, Bassaganyas L, Ramsay AJ, Bea S, Pinyol M, Martinez-Trillos A, et al. 2012. Exome sequencing identifies recurrent mutations of the splicing factor *SF3B1* gene in chronic lymphocytic leukemia. *Nat Genet* **44:** 47–52.

Radisky DC, Levy DD, Littlepage LE, Liu H, Nelson CM, Fata JE, Leake D, Godden EL, Albertson DG, Nieto MA, et al. 2005. Rac1b and reactive oxygen species mediate MMP-3-induced EMT and genomic instability. *Nature* **436:** 123–127.

Ramalingam S, Ramamoorthy P, Subramaniam D, Anant S. 2012. Reduced expression of RNA binding protein CELF2, a putative tumor suppressor gene in colon cancer. *Immunogastroenterology* **1:** 27–33.

Rhead B, Karolchik D, Kuhn RM, Hinrichs AS, Zweig AS, Fujita PA, Diekhans M, Smith KE, Rosenbloom KR, Raney BJ, et al. 2010. The UCSC Genome Browser database: update 2010. *Nucleic Acids Res* **38**(Database issue)**:** D613–D619.

Roovers K, Wagner S, Storbeck CJ, O'Reilly P, Lo V, Northey JJ, Chmielecki J, Muller WJ, Siegel PM, Sabourin LA. 2009. The Ste20-like kinase SLK is required for ErbB2-driven breast cancer cell motility. *Oncogene* **28:** 2839–2848.

Saito R, Smoot ME, Ono K, Ruscheinski J, Wang PL, Lotia S, Pico AR, Bader GD, Ideker T. 2012. A travel guide to Cytoscape plugins. *Nat Methods* **9:** 1069–1076.

Sanford JR, Wang X, Mort M, Vanduyn N, Cooper DN, Mooney SD, Edenberg HJ, Liu Y. 2009. Splicing factor SFRS1 recognizes a functionally diverse landscape of RNA transcripts. *Genome Res* **19:** 381–394.

Schneider CA, Rasband WS, Eliceiri KW. 2012. NIH Image to ImageJ: 25 years of image analysis. *Nat Methods* **9:** 671–675.

Seo JS, Ju YS, Lee WC, Shin JY, Lee JK, Bleazard T, Lee J, Jung YJ, Kim JO, Shin JY, et al. 2012. The transcriptional landscape and mutational profile of lung adenocarcinoma. *Genome Res* **22:** 2109–2119.

Shapiro IM, Cheng AW, Flytzanis NC, Balsamo M, Condeelis JS, Oktay MH, Burge CB, Gertler FB. 2011. An EMT–driven alternative splicing program occurs in human breast cancer and modulates cellular phenotype. *PLoS Genet* **7:** e1002218.

Singh A, Karnoub AE, Palmby TR, Lengyel E, Sondek J, Der CJ. 2004. Rac1b, a tumor associated, constitutively active Rac1 splice variant, promotes cellular transformation. *Oncogene* **23:** 9369–9380.

Spellman R, Llorian M, Smith CW. 2007. Crossregulation and functional redundancy between the splicing regulator PTB and its paralogs nPTB and ROD1. *Mol Cell* **27:** 420–434.

Srebrow A, Kornblihtt AR. 2006. The connection between splicing and cancer. *J Cell Sci* **119(**Pt 13**):** 2635–2641.

Thorsen K, Sorensen KD, Brems-Eskildsen AS, Modin C, Gaustadnes M, Hein AM, Kruhoffer M, Laurberg S, Borre M, Wang K, et al. 2008. Alternative splicing in colon, bladder, and prostate cancer identified by exon array analysis. *Mol Cell Proteomics* **7:** 1214–1224.

Tollervey JR, Curk T, Rogelj B, Briese M, Cereda M, Kayikci M, Konig J, Hortobagyi T, Nishimura AL, Zupunski V, et al. 2011. Characterizing the RNA targets and position-dependent splicing regulation by TDP-43. *Nat Neurosci* **14:** 452–458.

Venables JP, Klinck R, Koh C, Gervais-Bird J, Bramard A, Inkel L, Durand M, Couture S, Froehlich U, Lapointe E, et al. 2009. Cancer-associated regulation of alternative splicing. *Nat Struct Mol Biol* **16:** 670–676.

Venables JP, Brosseau JP, Gadea G, Klinck R, Prinos P, Beaulieu JF, Lapointe E, Durand M, Thibault P, Tremblay K, et al. 2013. RBFOX2 is an important regulator of mesenchymal tissue-specific splicing in both normal and cancer tissues. *Mol Cell Biol* **33:** 396–405.

Wang GS, Cooper TA. 2007. Splicing in disease: disruption of the splicing code and the decoding machinery. *Nat Rev Genet* **8:** 749–761.

Wang C, Norton JT, Ghosh S, Kim J, Fushimi K, Wu JY, Stack MS, Huang S. 2008a. Polypyrimidine tract-binding protein (PTB) differentially affects malignancy in a cell line-dependent manner. *J Biol Chem* **283:** 20277–20287.

Wang ET, Sandberg R, Luo S, Khrebtukova I, Zhang L, Mayr C, Kingsmore SF, Schroth GP, Burge CB. 2008b. Alternative isoform regulation in human tissue transcriptomes. *Nature* **456:** 470–476.

Wang Z, Kayikci M, Briese M, Zarnack K, Luscombe NM, Rot G, Zupan B, Curk T, Ule J. 2010. iCLIP predicts the dual splicing effects of TIA-RNA interactions. *PLoS Biol* **8:** e1000530.

Westhoff B, Colaluca IN, D'Ario G, Donzelli M, Tosoni D, Volorio S, Pelosi G, Spaggiari L, Mazzarol G, Viale G, et al. 2009. Alterations of the Notch pathway in lung cancer. *Proc Natl Acad Sci* **106:** 22293–22298.

Wood LD, Parsons DW, Jones S, Lin J, Sjoblom T, Leary RJ, Shen D, Boca SM, Barber T, Ptak J, et al. 2007. The genomic landscapes of human breast and colorectal cancers. *Science* **318:** 1108–1113.

Xiao X, Wang Z, Jang M, Nutiu R, Wang ET, Burge CB. 2009. Splice site strength–dependent activity and genetic buffering by poly-G runs. *Nat Struct Mol Biol* **16:** 1094–1100.

Xue Y, Zhou Y, Wu T, Zhu T, Ji X, Kwon YS, Zhang C, Yeo G, Black DL, Sun H, et al. 2009. Genome-wide analysis of PTB-RNA interactions reveals a strategy used by the general splicing repressor to modulate exon inclusion or skipping. *Mol Cell* **36:** 996–1006.

Xue Y, Ouyang K, Huang J, Zhou Y, Ouyang H, Li H, Wang G, Wu Q, Wei C, Bi Y, et al. 2013. Direct conversion of fibroblasts to neurons by reprogramming PTB-regulated microRNA circuits. *Cell* **152:** 82–96.

Yang W, Xia Y, Ji H, Zheng Y, Liang J, Huang W, Gao X, Aldape K, Lu Z. 2011. Nuclear PKM2 regulates β-catenin transactivation upon EGFR activation. *Nature* **480:** 118–122.

Yeo GW, Coufal NG, Liang TY, Peng GE, Fu XD, Gage FH. 2009. An RNA code for the FOX2 splicing regulator revealed by mapping RNA-protein interactions in stem cells. *Nat Struct Mol Biol* **16:** 130–137.

Yosef N, Ungar L, Zalckvar E, Kimchi A, Kupiec M, Ruppin E, Sharan R. 2009. Toward accurate reconstruction of functional protein networks. *Mol Syst Biol* **5:** 248.

Yosef N, Zalckvar E, Rubinstein AD, Homilius M, Atias N, Vardi L, Berman I, Zur H, Kimchi A, Ruppin E, et al. 2011. ANAT: a tool for constructing and analyzing functional protein networks. *Sci Signal* **4:** pl1.

Zhang J, Kong LM, Zhan R, Ye ZN, Pu JX, Sun HD, Li Y. 2014. Two natural *ent*-kauranoids as novel Wnt signaling inhibitors. *Nat Prod Bioprospect* **4:** 135–140.

Zhou C, Licciulli S, Avila JL, Cho M, Troutman S, Jiang P, Kossenkov AV, Showe LC, Liu Q, Vachani A, et al. 2013. The Rac1b splice form Rac1b promotes K-ras-induced lung tumorigenesis. *Oncogene* **32:** 903–909.

Zong FY, Fu X, Wei WJ, Luo YG, Heiner M, Cao LJ, Fang Z, Fang R, Lu D, Ji H, et al. 2014. The RNA-binding protein QKI suppresses cancer-associated aberrant splicing. *PLoS Genet* **10:** e1004289.

A network-based analysis of colon cancer splicing changes reveals a tumorigenesis-favoring regulatory pathway emanating from ELK1

Dror Hollander, Maya Donyo, Nir Atias, et al.

Supplemental Material	http://genome.cshlp.org/content/suppl/2016/02/11/gr.193169.115.DC1.html
References	This article cites 107 articles, 23 of which can be accessed free at: http://genome.cshlp.org/content/26/4/541.full.html#ref-list-1
Creative Commons License	This article is distributed exclusively by Cold Spring Harbor Laboratory Press for the first six months after the full-issue publication date (see http://genome.cshlp.org/site/misc/terms.xhtml). After six months, it is available under a Creative Commons License (Attribution-NonCommercial 4.0 International), as described at http://creativecommons.org/licenses/by-nc/4.0/.
Email Alerting Service	Receive free email alerts when new articles cite this article - sign up in the box at the top right corner of the article or **click here.**